Abnormal Regional and Global Connectivity Measures in Subjective Cognitive Decline Depending on Cerebral Amyloid Status

Shumei Li
German Center for Neurodegenerative Diseases, Bonn
Marcel Daamen
German Center for Neurodegenerative Diseases, Bonn
Lukas Scheef
German Center for Neurodegenerative Diseases, Bonn
Florian C. Gaertner
University Hospital Bonn, Department of Nuclear Medicine
Ralph Buchert
Charite Universitatsmedizin Berlin, Department of Nuclear Medicine
Martina Buchmann
German Center for Neurodegenerative Diseases, Tuebingen
Katharina Buerger
German Center for Neurodegenerative Diseases, Munich
Cihan Catak
Ludwig-Maximilians-Universitaet Muenchen, Institute for Stroke and Dementia Research (ISD)
Laura Dobisch
German Center for Neurodegenerative Diseases, Magdeburg
Alexander Drzezga
University Hospital of Cologne, Department of Nuclear Medicine
Birgit Ertl-Wagner
Ludwig-Maximilians-Universitat Muenchen, Institute for Clinical Radiology
Markus Essler
University Hospital Bonn, Department of Nuclear Medicine
Klaus Fliessbach
University Hospital Bonn, Department for Neurodegeneration and Geriatic Psychiatry
John Dylan Haynes
Charite Universitatsmedizin Berlin, Bernstein Center for Computational Neuroscience
Enise Irem Incesoy
German Center for Neurodegenerative Diseases, Berlin
Ingo Kilimann

German Center for Neurodegenerative Diseases, Rostock

Bernd J. Krause

University Medical Center Rostock, Department of Nuclear Medicine

Catharina Lange

Charite Universitaetsmedizin Berlin, Department of Nuclear Medicine

Christoph Laske

German Center for Neurodegenerative Diseases, Tuebingen

Josef Priller

German Center for Neurodegenerative Diseases, Berlin

Alfredo Ramirez

University of Cologne, Department of Psychiatry and Psychotherapy, Division of Neurogenetics and Molecular Psychiatry

Matthias Reimold

Eberhard-Karls-Universitaet Tuebingen, Department of Nuclear Medicine and Clinical Molecular Imaging

Axel Rominger

Ludwig-Maximilians-Universitaet Muenchen, Department of Nuclear Medicine

Nina Roy

German Center for Neurodegenerative Diseases, Bonn

Klaus Scheffler

University of Tuebingen, Department for Biomedical Magnetic Resonance

Angelika Schmitt

German Center for Neurodegenerative Diseases, Bonn

Anja Schneider

German Center for Neurodegenerative Diseases, Bonn

Annika Spottke

German Center for Neurodegenerative Diseases, Bonn

Eike Jakob Spruth

German Center for Neurodegenerative Diseases, Berlin

Stefan J. Teipel

German Center for Neurodegenerative Diseases, Rostock

Maike Tscheuschler

University of Cologne, Department of Psychiatry and Psychotherapy

Michael Wagner

German Center for Neurodegenerative Diseases, Bonn

Steffen Wolfsgruber

German Center of Neurodegenerative Diseases, Bonn

Emrah Düzel

German Center for Neurodegenerative Diseases, Magdeburg

Frank Jessen

University of Cologne,, Department of Psychiatry and Psychotherapy

Oliver Peters

German Center for Neurodegenerative Diseases, Berlin

Henning Boecker (**Henning.Boecker@dzne.de**)

https://orcid.org/0000-0003-2346-0598

Research

Keywords: [18F]-Florbetaben, PET, amyloid, subjective cognitive decline; DELCODE; precuneus, functional connectivity, compensatory mechanisms

Posted Date: February 13th, 2020

DOI: https://doi.org/10.21203/rs.2.23489/v1

Version of Record: A version of this preprint was published at Journal of Alzheimer's Disease on January 19th, 2021. See the published version at https://doi.org/10.3233/JAD-200472.

Abstract

Background: While cerebral beta-amyloid accumulation was found in many studies to alter precuneus-based functional connectivity (FC) in mild cognitive impairment and demented Alzheimer's disease (AD) patients, its impact is less well understood in subjective cognitive decline (SCD), which in the presence of underlying AD pathologic change corresponds to a progression to stage 2 of the clinical Alzheimer's continuum in the 2018 National Institute on Aging and Alzheimer's Association research framework, and represents the earliest clinical manifestation of AD.

Methods: From the DELCODE (DZNE – Longitudinal Cognitive Impairment and Dementia Study) cohort, two groups of 24 age- and gender-matched amyloid-positive SCD ($SCD_{A\beta+}$) and amyloid-negative SCD ($SCD_{A\beta-}$) patients were selected according to visual [18F]-Florbetaben PET readings, and studied with resting-state BOLD fMRI. Local (regional homogeneity (ReHo), amplitude of low-frequency fluctuation (ALFF) and fractional ALFF (fALFF)) and global (degree centrality (DC), precuneus seed-based FC maps) measures were calculated and compared between both groups. Furthermore, follow-up correlation analyses probed linear relationships of observed group differences with global as well as precuneal amyloid load measured by Florbetaben standard uptake value ratios ($SUVR_{FBB}$).

Results: For the local measures, ReHo was significantly higher in the bilateral precuneus for the $SCD_{A\beta+}$ group, whereas ALFF and fALFF measures were not altered between groups. For the global measures, relatively higher precuneus-based FC with occipital areas (but no altered DC) was observed in the $SCD_{A\beta+}$ group. Moreover, the FC differences between precuneus and occipital areas were positively correlated with global ($SCD_{A\beta+}$) and local precuneus $SUVR_{FBB}$ (both groups).

Conclusions: While confounding influences due to a higher ratio of APOE e4 carriers in the $SCD_{A\beta+}$ group cannot be excluded, results indicate functional alterations in the precuneus hub region that were linearly related to beta-amyloid load, highlighting incipient pathology and possible compensatory mechanisms in stage 2 of the AD continuum.

Background

Subjective cognitive decline (SCD) is increasingly acknowledged as the earliest symptomatic manifestation of Alzheimer's disease (AD) (1, 2). According to the conceptual framework for SCD research, subjective complaints include 'self-experienced persistent decline in cognitive capacity in comparison with a previously normal status and unrelated to an acute event', along with 'normal age-, gender-, and education-adjusted performance on standardized cognitive tests, which are used to classify mild cognitive impairment (MCI) or prodromal AD' (2). Although SCD is not specific for the presence of underlying AD pathology, an increased prevalence of preclinical AD cases has been reported in SCD complainers (3-5), providing support in favor of using the SCD concept as 'enrichment strategy' for

preclinical AD studies (2). Individuals with SCD and existing biomarker evidence for AD pathology were shown to be at increased risk of future cognitive decline, progression to MCI and, ultimately AD dementia (6-10). SCD with biomarker evidence of underlying AD pathologic change corresponds to stage 2 of the clinical AD continuum according to the novel NIA-AA (National Institute on Aging and Alzheimer's Association) working group criteria (11). According to recent meta-analytical evidence (12), available biomarker evidence for AD in combination with subtle cognitive decline is associated with an increased risk of clinical progression (73%), compared to asymptomatic amyloidosis alone (20%).

Brain functional alterations can be determined by functional connectivity (FC) analyses using resting-state functional magnetic resonance imaging (rs-fMRI), which is a sensitive tool for interrogating intrinsic functional connectivity properties and determining functional network disruptions as a consequence of underlying AD pathology. Functional connectivity alterations have been demonstrated in manifest AD dementia (13-16) and MCI (13, 17-19). Pertinent findings have been summed up in reviews and meta-analytical analyses (20-22), reporting AD stage-dependent FC alterations mainly in regions within default mode network (DMN), salience, and limbic networks (20, 23, 24). In the manifest AD stage, local [11C]-PiB (Pittsburgh Compound B) uptake in positron emission tomography (PET) correlates negatively with DMN connectivity (25), providing a direct link between amyloid load as a core pathological feature of AD and downstream functional readouts, although controversial findings were also reported (26). Amyloid load measured with PET in AD dementia /MCI is also linked with the fractional amplitude of low frequency fluctuation (fALFF), a marker for the strength / intensity of slow fluctuations in resting brain activity (26).

There is growing evidence that FC alterations already emerge during the preclinical stages of AD, and are linked with brain amyloid accumulation: The involvement of DMN structures is of special interest here, as its hub regions like the posterior cingulate cortex (PCC)/ precuneus appear particularly vulnerable to amyloid accumulation, and are among the first brain structures that show increasing amyloid tracer uptake in early amyloidosis (27). Various studies have described reductions of DMN connectivity in cognitively normal elderly with significant amyloid plaque depositions (28-30). Only subtle FC disruptions were observed in amyloid-positive asymptomatic older individuals by Drzezga et al. (31), whereas amyloid-positive MCI showed significant disruptions of whole-brain FC in 'typical cortical hubs' like the PCC/precuneus, suggesting incipient functional deterioration. Meanwhile, there are also studies showing FC increases (32), or mixed patterns of FC increases and decreases (33), which may represent functional shifts within and between FC networks that are related to amyloid accumulations (34).

Building on the assumption that SCD patients are at-risk for preclinical AD, a variety of studies started to explore whether AD-related patterns of FC alterations (especially in DMN areas) are already observable here (35-39). Hafkemeijer et al. (40) reported increased FC in DMN (and medial visual) areas, including PCC and precuneus, in elderly SCD, as compared to age-matched controls. Yasuno et al. (41) compared seed-based FC among cortical midline structures (featuring several DMN core nodes), and reported reduced FC especially for bilateral retrosplenial cortex seeds in SCD compared to healthy control. Dong et al. (42) found a reduction in global absolute FC strength for SCD participants (based on informant reports) in fronto-parieto/occipital regions (left medial superior frontal, left precuneus, left parietal, right

cuneus, and bilateral calcarine cortex) along with an increase in relative FC strength in posterior cingulate cortex/precuneus. Another recent study (43) in asymptomatic subjects with a family history of AD described increased FC between the posterior DMN and medial temporal areas in individuals with SCD, as compared to non-complainers. In contrast, Viviano et al. (44) observed reduced average connectivity among posterior (especially between precuneus and retrosplenial cortex), but not among anterior memory system nodes. Chiesa et al. (45) analyzed longitudinal DMN connectivity changes over 24 months, and observed widespread FC increases (along with limited decreases in dorsal aspects of the precuneus) within a large cohort of SCD individuals.

To some degree, the variability of available FC finding may relate to the fact that most of these studies examined SCD patients without stratifying by AD biomarker status, i.e. actual FC changes related to preclinical AD pathology in SCD populations may be obscured by varying proportions of participants with SCD due to non-AD mechanisms. For example, Yasuno et al. (41) reported that among 13 SCD participants who performed amyloid PET, only one was classified amyloid-positive (but see: (45)). Likewise, there is very limited data examining possible correlations between amyloid biomarkers and FC measures in SCD populations directly: While Yasuno et al. (41) found no relationships between the observed FC alterations and amyloid tracer uptake, Li et al. (46) observed increased degree centrality (DC) of the bilateral hippocampus and left fusiform area in 44 individuals with subjective memory complaints, as compared with 40 normal controls, to be positively correlated with cerebrospinal fluid (CSF) total and phosphorylated tau (but not amyloid) levels.

Here, we report data from DELCODE (DZNE – Longitudinal Cognitive Impairment and Dementia Study), which is an ongoing observational longitudinal multicenter study focusing on SCD (47). Considering (i) that most of the abovementioned studies were not specifically targeted on SCD as early clinical manifestation of possible AD, (ii) that few studies in the SCD stage were informed by amyloid biomarker status, and (iii) that the precuneus is an important hub region of the posterior DMN showing a high vulnerability for amyloid depositions (48, 49), this study specifically addressed the question how amyloid pathology relates to several local and global measures of rs-fMRI in SCD patients exclusively recruited from memory clinics. The focus of this study is on the precuneus. While an initial analysis from this cohort (18) found no FC alterations that differentiated SCD from healthy controls, this preliminary subsample did not include enough SCD with proven amyloid pathology (SCD_{Ab+}, as measured by cerebrospinal fluid [CSF]) to systematically examine specific alterations in this subgroup, as compared to healthy controls, or SCD without amyloid pathology (SCD_{Ab-}). Here, we used qualitative ratings from amyloid PET examinations to directly compare 24 SCD_{Ab+} with 24 age- and sex-matched SCD_{Ab-} participants (see also: (42)). We hypothesized (i) precuneus-based FC changes and alterations of regional measures to occur in SCD_{Ab+}, as compared to SCD_{Ab-}, and (ii) these changes to correlate with the severity of global and regional precuneus Aβ load which we examined in additional, exploratory analyses. The direction of respective changes was not predicted *a priori*, based on equivocal findings in the available literature in SCD patients.

Methods

General procedures

All participants in this study were taken from the PET sub-cohort of the DELCODE study, whose overall study design and detailed inclusion and exclusion criteria have been described elsewhere (47). Based on qualitative visual readings of [18F]-Florbetaben (FBB, Neuraceq^{TM}: Life Radiopharma Berlin GmbH) PET scans, the first 24 SCD_{Ab+} individuals with significant cerebral amyloid depositions and valid rs-fMRI data were compared with a respective group of 24 age- and sex-matched SCD_{Ab-} participants without significant cerebral amyloid depositions.

Sample characteristics

Further details about sample characterization can be found elsewhere (47). In brief, all DELCODE study participants complete extensive neuropsychological testing during the yearly study visits, including the Mini Mental State Examination (MMSE: (50)), and a modified version of the Alzheimer's Disease Assessment Scale-Cognitive-Plus (ADAS-Cog-13: (51)). Apolipoprotein (APOE) genotyping was performed using commercially available TaqMan® SNP Genotyping Assay (ThermoFisher Scientific).

[18F]-Florbetaben PET acquisition

PET data were acquired on clinical PET/CT or PET/MR scanners at the nuclear medicine departments of the participating sites (Table S1). Data acquisition followed established standard procedures for FBB scanning: After intravenous FBB tracer application of 282 ± 9 MBq, dynamic 3D-acquisition of list mode emission data started 90.9 ± 3.6 min post-injection, for a total duration of 20 minutes (which were subsequently reconstructed into 4 x 5 min time frames). Additionally, low-dose CT (or for PET/MR: 3D Dixon-VIBE sequences) were collected for calculation of attenuation correction maps. Iterative reconstruction was performed based on the established PET brain protocols at the local sites, including decay, random, scatter, dead time, normalization, and attenuation correction.

[18F]-Florbetaben PET analyses

Qualitative analysis: As the current gold-standard, visual readings of the [18F]-Florbetaben (FBB) scans were conducted by two experienced readers (HB, FG) according to manufacturer guidelines (52), resulting in a consensus rating of amyloid positivity (SCD_{Ab+}) and amyloid negativity (SCD_{Ab-}) which was used for group definition.

Quantitative analysis: To explore potential linear relationships between the severity of cortical amyloid load and rs-fMRI measures, we conducted secondary quantitative analyses. Using the PNEURO Maximum Probability Atlas pipeline in PMOD 4.004 (PMOD Technologies LLC, Zurich, Switzerland), PET images series were motion-corrected and coregistered with a T1-weighted anatomical scan of the participant (see below) which was segmented using Unified Segmentation (53). Normalization parameters from this segmentation were used to warp the AAL atlas template (54) into participants' native PET space, where

the transformed AAL volume of interest (VOI) definitions were additionally masked by thresholding the individual gray matter (GM), white matter (WM) and cerebrospinal fluid (CSF) probability maps. Within each VOI, standard uptake values (SUV) were averaged across voxels and time frames. Similar to Barthel et al. (55), a volume-weighted average of bilateral frontal, lateral temporal, parietal, occipital and cingulate SUV was calculated, and scaled by tracer uptake in the cerebellar cortex to derive a global SUV ratio ($SUVR_{FBB}$) for measuring global Aβ load. The same procedure was applied to left and right precuneus VOI to derive regional $SUVR_{FBB}$ for the bilateral precuneus.

MRI acquisition

MRI data acquisition was performed on 3 Tesla Siemens scanners from seven scanning sites across Germany, using harmonized imaging sequences across sites. The rs-FMRI data were acquired axially using an echo-planar imaging (EPI) sequence with the following sequence parameters: TR/TE = 2580/ 30 ms, flip angle: 80°, field of view = 224 × 224 mm^2, resolution = 64 × 64 matrix, number of slices = 47, slice thickness = 3.5 mm, total of 180 volumes, acquisition time approximately 8 min. During the examination, subjects were instructed to hold still, keep their eyes closed, not to fall asleep, and not to think of anything in particular. For registration purposes, T1-weighted magnetization-prepared rapid gradient echo sequence (MPRAGE) sequences were acquired (TR: 2500ms, TE: 4.37ms, flip angle: 7°, TI: 1100ms, GRAPPA = 2, 256 × 256 matrix, FOV: 256 x 256 mm^2, slice thickness: 1mm, 192 sagittal sections, no gap).

rs-fMRI data preprocessing

The rs-fMRI data preprocessing steps were conducted using the Data Processing & Analysis for Brain Imaging (DPABI) toolbox (56) in Matlab 2015a (MathWorks, Inc., Natick, MA). The first 5 EPI volumes were discarded to account for transient signal changes before magnetization reached a steady-state. The remaining 175 EPI volumes were corrected for different signal acquisition times and head movements. The T1-weighted images were co-registered to the mean of the realigned functional images series, and segmented into GM, WM and CSF (53). Nuisance covariates including 24 motion parameters (57), white matter and CSF mean time course signals were regressed out. In addition, a motion scrubbing regressor method (58) was used for each bad time point (frame-wise displacement > 0.2 mm included as covariate). The images were normalized into ICBM-152 reference space using DARTEL (Diffeomorphic Anatomical Registration Through Exponentiated Lie Algebra: (59)). According to previous studies, spatial smoothing was performed with a Gaussian kernel of 6 mm full-width at half-maximum (FWHM) before ALFF, fALFF and FC calculation (60), but after ReHo and degree centrality (DC) calculation (61). Finally, temporal band-pass filtering (0.01–0.08 Hz) was adopted to reduce the effect of low-frequency drifts and high-frequency physiological noise before ReHo and DC calculation, but after ALFF and fALFF calculation.

Regional Homogeneity (ReHo) calculation

ReHo represents a voxel-based measure of brain activity which evaluates the local synchronization between the time series of a given voxel and its nearest neighbors (62). We used DPABI to obtain each

subject's ReHo map by calculating Kendall's coefficient of concordance for a given voxel time series with its nearest 26 neighboring voxels. This analysis was based on the unsmoothed preprocessed images (62). To improve comparability between subjects, standard normal z transformation was applied to all ReHo maps. Finally, these 'zReHo maps' were spatially smoothed with a 6 mm FWHM Gaussian kernel for the following statistical analysis.

Amplitude of Low Frequency (ALFF) and fractional ALFF calculation

ALFF is defined as the total power within the low frequency range (0.01-0.08 Hz) and represents the strength or intensity of low frequency oscillations (LFO), while fALFF is defined as the power within the low-frequency range divided by the total power in the entire detectable frequency range and represents the relative contribution of specific LFO to the whole frequency range (63). Individual ALFF maps were calculated using DPABI, as described previously (64). The functional time series of each voxel was transformed to the frequency domain using a fast Fourier transform algorithm and the power spectrum was obtained. As the power of a given frequency is proportional to the square of the amplitude of this frequency component, the square root was calculated at each frequency of the power spectrum and the averaged square root was obtained across 0.01–0.08 Hz at each voxel. This averaged square root was taken as the ALFF value (64). Moreover, fALFF was calculated using the ratio of power spectrum of low-frequency (0.01 Hz to 0.08 Hz) to that of the entire frequency range. For statistical analysis, standard normal z-transformation was applied to all ALFF and fALFF maps (to generate the zALFF and zfALFF maps).

Degree Centrality (DC) calculation

DC represents the number of direct connections for a given voxel in voxel-based graphs (65) and has been widely used to represent the node property of large-scale brain networks. DC maps were calculated as described previously (66) using DPABI. Specifically, we calculated Pearson's correlations between the time course of any pair of voxels within the whole brain to generate the functional connectivity matrix. We obtained each subject's undirected adjacency matrix by thresholding each correlation at $r>0.25$, in order to exclude voxels that had low temporal correlation attributable to signal noise (65). Standard normal z transformation was applied to each DC map to generate the zDC map. Finally, the zDC maps were spatially smoothed with a 6 mm FWHM Gaussian kernel for the following statistical analysis.

Voxel-based Bilateral Precuneus FC Analysis

FC analysis of the bilateral precuneus was conducted in voxel-wise manner. The seed region, bilateral precuneus, was generated from the AAL atlas, multiplied with the GM mask. Voxel-wise FC map was calculated using the correlations between the mean time series of the seed region and remaining voxels within the brain. To improve the normality of FC correlation coefficient maps, the correlation coefficients were converted to z values using Fisher's transformation.

Statistical analyses

Statistical analyses were performed with SPM12 (Wellcome Department of Cognitive Neurology, London) and SPSS 22.0 (IBM Corp.: Armonk, NY). For background characteristics of the sample, group differences were assessed using independent sample t-, Mann-Whitney U-, or chi-squared tests ($p<0.05$). For the voxel-wise FC, ReHo, ALFF/fALFF and DC differences between groups, a second-level two-sample t-test was performed on the individual maps in a voxel-by-voxel manner. The results were considered significant at $p<0.05$, family-wise error (FWE) corrected at cluster level, based on a voxel-level threshold $p<0.01$. To examine linear relationships with global or regional Aβ load, Pearson correlations were calculated between mean FC values in clusters showing significant group differences between $SCD_{Aβ+}$ and $SCD_{Aβ-}$ and (i) precuneus and (ii) global $SUVR_{FBB}$, respectively.

Results

Sample characteristics and Amyloid SUVRs

Descriptive statistics of background characteristics for the $SCD_{Aβ+}$ and $SCD_{Aβ-}$ samples are presented in Table 1, showing no significant group differences, except for a higher proportion of APOE e4 carriers in the $SCD_{Aβ+}$. As expected, the global $SUVR_{FBB}$ and the regional precuneus $SUVR_{FBB}$ was significantly higher in the $SCD_{Aβ+}$ compared to the $SCD_{Aβ-}$ group. Yet, we note that several participants in both subgroups showed global SUVR values borderline to previous FBB SUVR cut-off definitions for amyloid positivity, resulting in slightly varying amyloid-positivity classifications. Using $SUVR_{global}$ = 1.39 from Barthel et al. (55), N=1 $SCD_{Aβ+}$ would be classified amyloid-negative, while N=5 $SCD_{Aβ-}$ would be classified amyloid-positive.

Group comparison: Local rs-fMRI metrics

The voxel-based ReHo analysis revealed significantly increased ReHo in the bilateral precuneus and the adjacent superior parietal lobule in the $SCD_{Aβ+}$, as compared to the $SCD_{Aβ-}$ group (Table 2, Figure 1). On the other hand, no significant group differences were found in ALFF/ fALFF and in DC.

Group comparison: Global rs-fMRI metrics

Voxel-wise FC analysis revealed that the $SCD_{Aβ+}$ group showed an increased FC between the precuneus mean time course and occipital regions, including the superior occipital gyrus and the bilateral cuneus (Table 3, Figure 2).

Possible influence of nuisance variables:

To test for possible effects of (a) different MR sites on rs-fMRI measures in this multi-center study and (b) the highly significant group differences in APOE genotype, additional second-level two-sample t-tests with MR scanners (dummy-coded) and APOE status (e4+/e4-) as additional covariates were performed. For ReHo, these analyses yielded slightly weaker findings (likely due to the reduced degrees of freedom), but left-sided group differences were still significant (Figure S1), indicating that pertinent findings were not

primarily influenced by scanner effects or APOE status. As for the precuneus-FC findings, this analysis rendered the reported group differences nonsignificant, suggesting that confounding influence of APOE genotype cannot be excluded, as significant group differences were still evident in a separate model controlling for MR scanners only (Figure S2).

Exploratory analyses: Associations of FC differences with quantitative amyloid load

No significant association was found between the global and/or local precuneus $SUVR_{FBB}$ and the mean z-score of the ReHo extracted from the precuneus cluster that showed the significant group difference between the $SCD_{A\beta+}$ and $SCD_{A\beta-}$ groups.

On the other hand, the mean z-score of the FC extracted from the superior occipital gyrus and the bilateral cuneus (showing significant group differences) was positively correlated with global $SUVR_{FBB}$ in the $SCD_{A\beta+}$ ($r_{A\beta}{}^{+}$ =0.495, p=0.014) but not in the $SCD_{A\beta-}$ ($r_{A\beta-}$= -0.012, p=0.926) group, with a significant difference between the correlation coefficients for the two groups (z = 1.82, p = 0.034), as well as with the regional precuneus $SUVR_{FBB}$ in both $SCD_{A\beta+}$ ($r_{A\beta+}$= 0.45, p=0.027) and $SCD_{A\beta-}$ ($r_{A\beta-}$= 0.474, p=0.039) individuals (Figure 3), which was not significantly different between groups (z = -0.098, p = 0.461).

Discussion

Our study, focusing on the SCD sub-cohort of DELCODE explored precuneus-based whole-brain FC and several regional and global measures of rs-fMRI changes in matched $SCD_{A\beta+}$ compared to the $SCD_{A\beta-}$ groups. Additionally, we studied the relationship between the rs-fMRI measures and global/ precuneus Aβ load. The key findings were a demonstration of increased ReHo in bilateral precuneus and adjacent superior parietal gyrus in the $SCD_{A\beta+}$ group, as compared to the $SCD_{A\beta-}$ group (Figure 1), but no significant difference regarding ALFF / fALFF and DC measures. Moreover, $SCD_{A\beta+,}$ as compared to $SCD_{A\beta-}$ participants, were characterized by increased precuneus FC with occipital regions (Figure 2). While confounding influences of group differences regarding APOE genotype cannot be excluded, the additional observation (Figure 3) that FC increases between precuneus and occipital areas showed positive linear associations with global ($SCD_{A\beta+}$) as well as local precuneus amyloid load ($SCD_{A\beta+}$ and $SCD_{A\beta-}$) argues for gradual connectivity changes that are partially related to incipient accumulation of amyloid pathology.

Several previous studies have shown associations of Aβ accumulation not only with decreased, but also with increased connectivity in nondemented populations (32, 33). However, as yet the functional consequences resulting from elevated amyloid burden in the SCD stage remain unsolved. The precuneus was of particular interest for this study as this region is known to be vulnerable for early Aβ deposition (67), with higher Aβ deposition being found in both, AD (65) and MCI (68). A recent study in elderly healthy controls, SCD and MCI patients provided further proof that Aβ accumulation preferentially starts in the precuneus, along with medial orbitofrontal, and PCC (27).

Our results showed increased bilateral precuneus FC with adjacent occipital areas in $SCD_{Aβ+}$, which is partially consistent with a study (30) observing stronger precuneus-occipital connectivity in Aβ+ (as compared to Aβ-) cognitively normal participants. There are also parallels with previous work (40) using independent component analysis (ICA) with dual regression to investigate resting-state FC: Compared with age-matched controls, patients with subjective memory complaints showed increased FC within the DMN and medial visual network. Unfortunately, these group comparisons were not informed by amyloid biomarker information. In a recent paper investigating individuals with a family history of AD (43), increased FC of the posterior DMN (PCC) with the medial temporal memory system was found in participants who were complaining about SCD (as compared to non-complainers). Yet, SCD classification was only based on a single questionnaire item examining subjective worsening of memory, and AD pathology was not scrutinized by AD biomarkers. Interestingly, previous studies in cognitively normal individuals also reported posterior DMN hyperconnectivity to be correlated with AD risk factors and, hence, could represent an early compensatory mechanism to overcome cognitive decline (32, 69-71). These findings are supported and further extended by the current study: The observed higher connectivity of the precuneus with the occipital gyrus, qualified by the positive association between FC in occipital regions and regional precuneus Aβ load may indeed reflect a local compensatory mechanism at an early pathophysiological stage that helps to maintain normal behavioral performance in $SCD_{Aβ+}$. In this context, a recent publication by Schultz et al. (72) is of particular relevance: The authors reported increased FC in the DMN (and the salience network) in Aβ+ clinically normal individuals with low neocortical tau, while on the other hand, FC was decreased in Aβ+ clinically normal individuals with elevated neocortical tau-PET signal. Their findings suggesting ‘a hyperconnectivity phase followed by a hypoconnectivity phase in the course of preclinical AD’ (p. 4323) is highly interesting in the context of the current study and might suggest that the majority of $SCD_{Aβ+}$ individuals were not yet tau-positive. Unfortunately, we had no tau PET data available to test this assumption. Nonetheless, the suggested sequential phases of FC changes are compatible with a transitional phase of compensation that later breaks down during the course of disease.

Interestingly, the positive association between precuneus-occipital FC and global $SUVR_{FBB}$ values was only visible in the $SCD_{Aβ+}$ subgroup, while a positive correlation with the precuneus $SUVR_{FBB}$ also emerged in the $SCD_{Aβ-}$ subgroup. This may indicate that these FC changes are mainly driven by incipient local (=precuneus) amyloid accumulations which are masked in global composites. Complementary evidence for regional specificity comes from a mixed population of SCD and healthy controls (73) who had negative amyloid PET scans (according to visual reading and global cortical SUVR cut-offs) but showed positive correlations between dynamic whole-brain connectivity measures and SUVR values from brain areas with early amyloid accumulation (including PCC and precuneus: see (48)). These relationships were not evident when using complementary SUVR values from an entire DMN, or global cortical mask.

No significant differences between $SCD_{Aβ+}$ and $SCD_{Aβ-}$ were found for the ALFF/fALFF and DC measures. Although both, ReHo and ALFF/fALFF measures reflect brain regional spontaneous neuronal activity,

there are considerable differences with ReHo which reflects similarity of spontaneous neuronal activity among nearby voxels. Therefore, our results may suggest ReHo to be a more sensitive measure for detecting early local brain activity alterations interpreted as a functional compensation mechanism for enhancing regional coherence of neuronal activity. Our non-significant results regarding DC, which is a measure based on graph theory, may indicate that brain function at the network level is still not altered in the $SCD_{A\beta+}$ group, as compared to the $SCD_{A\beta-}$ group.

The observation of higher precuneal ReHo and FC in $SCD_{A\beta+,}$ compared to $SCD_{A\beta-}$, may correspond to elevated compensation in a very early stage of preclinical AD (33, 40, 43) where additional neuronal processing is required to balance the brain workload, thereby, maintaining normal cognitive functioning. Yet, in a mechanistic sense, Aβ pathology may also be accelerated by increased metabolism and elevated intrinsic activity / connectivity (31, 74, 75), with laboratory evidence indicating that neuronal activity directly increases production of Aβ peptides (76). Considering that the precuneus is a prominent 'hub' in the intrinsic FC matrix of the human brain and metabolically active (77), our finding of relatively higher connectivity and ReHo within this region might indeed trigger (or amplify) Aβ production in $SCD_{A\beta+.}$

Due the significantly higher rate of APOE e4 carriers in the amyloid-positive group, which is not unexpected given the frequently observed association between APOE genotype and amyloidosis (78), it is difficult to disentangle the relative contributions of amyloid positivity *per se* and APOE genotype, to FC group differences. While left-sided ReHo group differences survived even after controlling for APOE status (Figure S1), precuneal-FC group differences were rendered non-significant. The available sample size precluded further stratifications according to APOE status. While APOE genotype was shown to have independent effects on FC measures, even in individuals whose amyloid PET was negative (34, 69, 79), its influence may also be indirectly mediated by its effect on amyloid accumulation. Actually, the observed linear association between quantitative amyloid load, especially in the precuneus, and precuneal FC with the occipital region (Figure 3), would support the latter interpretation.

Some methodological limitations need to be considered. First, the relatively small sample size in this study limits statistical power. Future studies with larger sample sizes will have to be awaited to validate the findings in this study. Second, the present analyses were restricted to cross-sectional rs-fMRI data, precluding inferences about the longitudinal course of the amyloid-related FC changes: In fact, the longitudinal DMN connectivity changes observed by Chiesa et al. (45) were partially linked to APOE genotype, but not to amyloid positivity. Third, we have to acknowledge that the relationship between early brain functional alterations and longitudinal declines in neuropsychological test performance will need to be explored in future studies, as collection of follow-up data is ongoing. For example, Buckley et al. (80) reported that lower FC particularly of DMN, salience, and control networks predicted more rapid cognitive decline in normal older adults with increased Aβ burden, suggesting that FC measures add predictive information about cognitive trajectories. Fourth, we had no access to a healthy control group with (PET-) proven amyloid-negativity to characterize relative FC differences in $SCD_{A\beta+}$, and to make clear statements whether FC increases reflect a state of true hyperconnectivity. Fifth, recent evidence for interaction effects regarding sex (81) could not be tested systematically due to the limited sample size. Yet, our comparison

of $SCD_{Aβ+}$ with sex-matched $SCD_{Aβ-}$ participants assured that this potential confounds could not bias group comparisons. Sixth, visual reading vs. application of previously established global SUVR cut-offs does not result in entirely consistent amyloid status classifications. In general, recent data indicate that the correspondence between FBB visual reading and classification with global SUVR cut-offs is high (>85%), yet not perfect (82). Moreover, the global SUVR for a substantial number of participants were in proximity around the respective cut-off values, suggesting a continuum of intermediate amyloid deposition states which are more difficult to classify reliably. On the other hand, this observation provides further support for our exploratory linear correlation analyses with the SUVR measures. Finally, we did not have access to tau-PET data in this cohort and we are, thus, not able to unravel whether precuneus FC is affected additionally by elevated tau, as hypothesized by previous work (72). Therefore, further studies will have to be awaited to further explore the FC changes in SCD with complementary amyloid and tau biomarker information.

Conclusions

In summary, our study in well-matched SCD cohorts differing in PET-proven cerebral amyloid pathology provides an important addition to the previous literature, namely by demonstrating increased local precuneus (ReHo) and global (higher precuneus-based FC with occipital areas) FC measures in $SCD_{Aß+}$ compared to $SCD_{Aβ-}$ individuals. Our results indicate vulnerability of precuneal neural activity in the SCD stage with positive biomarker evidence for amyloid pathology (NIA-AA stage 2 of the clinical AD continuum) and suggest FC changes in this important hub region to be directly linked to concurrent amyloid pathology. Combined with the positive linear association of the FC between the precuneus and occipital regions with cortical amyloid load, our findings suggest compensatory brain functional mechanisms to overcome early amyloid pathology in the SCD stage. Resting-state FC appears to be a useful neuroimaging biomarker for highlighting early brain functional consequences of AD pathology.

Declarations

Ethics approval and consent to participation:

DELCODE and DELCODE-PET were approved by the institutional review boards of all participating sites (Charité Berlin, Bonn, Cologne, Ludwig-Maximilians-University Munich, Rostock, and Tübingen), and coordinated by the ethics committee of the medical faculty of the University of Bonn, under the registration numbers: 117/13 (DELCODE) and 221/13 (DELCODE-PET). DELCODE-PET was also approved by the federal radiation protection authority (Bundesamt für Strahlenschutz). All procedures were performed in accordance with the relevant guidelines and regulations. All participants provided written informed consent.

Consent for publication:

Not applicable

Availability of data and materials:

The data which support this study are not publicly available, but may be provided upon reasonable request.

Competing interests:

KB is advisor for Biogen GmbH. The other authors report no conflicts of interest relevant for this study.

Funding:

The study was funded by the German Center for Neurodegenerative Diseases (Deutsches Zentrum für Neurodegenerative Erkrankungen, DZNE), Reference number BN012.

The analyses of the Florbetaben PET exams reported in this study are subject of a research agreement with Life Molecular Imaging.

Authors' contributions:

The following authors contributed to the overall design and implementation of DELCODE-PET: HB, FJ, A. Spottke, MD, A. Schmitt, NR. The following authors were responsible for conducting the DELCODE and/ or DELCODE-PET study examinations at the respective sites: OP, EII, JP, EJS, CL, RB, JDH, A. Schneider, KF, ME, FCG, FJ, MT, AD, KB, CC, A. Rominger, BEW, SJT, IK, BJK, CL, MB, MR, KS. The following authors were responsible for methodological core data management and analyses: ED, LD, MW, SW, A. Ramirez. The following authors were responsible for the Florbetaben visual ratings: FCG, HB. The following authors were responsible for data analyses, data interpretation, and drafting of the manuscript: SL, MD, LS, HB. All authors read and approved the final manuscript.

Acknowledgements:

The authors would like to thank the Max Delbrück Center for Molecular Medicine in the Helmholtz Society (MDC), the Center for Cognitive Neuroscience Berlin at the Freie Universität Berlin (CCNB) and, especially, the DELCODE participants and their families.

DELCODE Study Group:

S. Altenstein, H. Amthauer, A. Bader, M. Barkhoff, M. Beuth, H. Boecker, F. Brosseron, K. Brüggen, M. Buchmann, K. Buerger, C. Catak, L. Coloma Andrews, M. Daamen, S. de Jonge, M. Dichgans, A. Dörr, M. Dyrba, M. Ehrlich, T. Engels, B. Ertl-Wagner, C. Escher, J. Faber, K. Fliessbach, D. Frimmer, I. Frommann, M. Fuentes , N. Ghiasi, D. Hauser, T. Heger, C. Heine, J. Henf, G. Hennes, G. Herrmann, P. Hinderer, B. Huber, A. Hufen, H. Janecek-Meyer, D. Janowitz, F. Jessen, K. Kafali, C. Kainz, P. Kalbhen, E. Kasper, I. Kilimann, X. Kobeleva, B. Kofler, C. Korp, M. Kreuzer, E. Kuder-Buletta, C. Kurz, A. Langenfurth , C. Laske, E. Lau, K. Lindner, A. Lohse, H. Lützerath, F. Maier, E. Markov, B. Marquardt, A. Martikke, H. Megges, D. Meiberth, F. Menne, L. Miebach, A. Müller, C. Müller, C. Mychajliw, O. Peters, H. Pfaff, A. Polcher, J. Priller, H. Raum, A.

Rominger, S. Röske, A. Rostamzadeh, P. Sabik, Y. Sagik, P. Sänger, L. Sannemann, A.-K. Schild, J. Schmid, M. Schmidt, A. Schmitt, C. Schneider, A. Schneider, H. Schulz, S. Schwarzenboeck, A. Seegerer, S. Sorgalla, A. Spottke, E. J. Spruth, J. Stephan, A. Szagarus, S. J. Teipel, M. Thelen, M. Tscheuschler, I. Villar Munoz , I. Vogt, M. Wagner, M. Weber, S. Weschke, C. Westerteicher, C. Widmann, S. Wolfsgruber, A. Zollver.

Abbreviations

AAL Automated Anatomical Labeling

Aβ+/ Aβ- Beta-amyloid positive/ negative

AD Alzheimer's Disease

ADAS-cog-13 Alzheimer's Disease Assessment Scale-Cognitive-Plus

APOE Apolipoprotein

CSF Cerebrospinal fluid

CT Computer Tomography

DARTEL Diffeomorphic Anatomical Registration Through Exponentiated Lie Algebra

DC Degree centrality

DELCODE DZNE – Longitudinal Cognitive Impairment and Dementia Study

DMN Default Mode Network

DPABI Data Processing & Analysis for Brain Imaging

EPI Echo-planar Imaging

(f)ALFF (Fractional) Amplitude of Low Frequency Fluctuation

FBB [18F]-Florbetaben

FC Functional Connectivity

FOV Field Of View

FWE Family-wise Error

GM Grey matter

GRAPPA Generalized Autocalibrating Partial Parallel Acquisition

LFO Low Frequency Oscillations

MCI Mild Cognitive Impairment

MMSE Mini Mental State Examination

MPRAGE Magnetization-Prepared Rapid Gradient Echo

MR(I) Magnetic Resonance (Imaging)

NIA-AA National Institute on Aging and Alzheimer’s Association

PCC Posterior Cingulate Cortex

PET Positron Emission Tomography

PiB Pittsburgh Compound B

ReHo Regional Homogeneity

rs-fMRI Resting-State functional Magnetic Resonance Imaging

SCD Subjective Cognitive Decline

SUV(R) Standard Uptake Value (Ratio)

TE Echo time

TI Inversion Time

TR Repetition time

VOI Volume of Interest

WM White matter

References

1. Buckley RF, Villemagne VL, Masters CL, Ellis KA, Rowe CC, Johnson K, et al. A Conceptualization of the Utility of Subjective Cognitive Decline in Clinical Trials of Preclinical Alzheimer's Disease. J Mol Neurosci. 2016;60(3):354-61.
2. Jessen F, Amariglio RE, van Boxtel M, Breteler M, Ceccaldi M, Chetelat G, et al. A conceptual framework for research on subjective cognitive decline in preclinical Alzheimer's disease. Alzheimers Dement. 2014;10(6):844-52.

3. Visser PJ, Verhey F, Knol DL, Scheltens P, Wahlund LO, Freund-Levi Y, et al. Prevalence and prognostic value of CSF markers of Alzheimer's disease pathology in patients with subjective cognitive impairment or mild cognitive impairment in the DESCRIPA study: a prospective cohort study. Lancet Neurol. 2009;8(7):619-27.
4. Mosconi L, De Santi S, Brys M, Tsui WH, Pirraglia E, Glodzik-Sobanska L, et al. Hypometabolism and altered cerebrospinal fluid markers in normal apolipoprotein E E4 carriers with subjective memory complaints. Biol Psychiatry. 2008;63(6):609-18.
5. Rami L, Fortea J, Bosch B, Sole-Padulles C, Llado A, Iranzo A, et al. Cerebrospinal fluid biomarkers and memory present distinct associations along the continuum from healthy subjects to AD patients. J Alzheimers Dis. 2011;23(2):319-26.
6. Prichep LS, John ER, Ferris SH, Rausch L, Fang Z, Cancro R, et al. Prediction of longitudinal cognitive decline in normal elderly with subjective complaints using electrophysiological imaging. Neurobiol Aging. 2006;27(3):471-81.
7. van Harten AC, Visser PJ, Pijnenburg YA, Teunissen CE, Blankenstein MA, Scheltens P, et al. Cerebrospinal fluid Abeta42 is the best predictor of clinical progression in patients with subjective complaints. Alzheimers Dement. 2013;9(5):481-7.
8. Eckerstrom M, Gothlin M, Rolstad S, Hessen E, Eckerstrom C, Nordlund A, et al. Longitudinal evaluation of criteria for subjective cognitive decline and preclinical Alzheimer's disease in a memory clinic sample. Alzheimers Dement (Amst). 2017;8:96-107.
9. Amariglio RE, Buckley RF, Mormino EC, Marshall GA, Johnson KA, Rentz DM, et al. Amyloid-associated increases in longitudinal report of subjective cognitive complaints. Alzheimers Dement (N Y). 2018;4:444-9.
10. Vogel JW, Varga Dolezalova M, La Joie R, Marks SM, Schwimmer HD, Landau SM, et al. Subjective cognitive decline and beta-amyloid burden predict cognitive change in healthy elderly. Neurology. 2017;89(19):2002-9.
11. Jack CR, Jr., Bennett DA, Blennow K, Carrillo MC, Dunn B, Haeberlein SB, et al. NIA-AA Research Framework: Toward a biological definition of Alzheimer's disease. Alzheimers Dement. 2018;14(4):535-62.
12. Parnetti L, Chipi E, Salvadori N, D'Andrea K, Eusebi P. Prevalence and risk of progression of preclinical Alzheimer's disease stages: a systematic review and meta-analysis. Alzheimers Res Ther. 2019;11(1):7.
13. Gili T, Cercignani M, Serra L, Perri R, Giove F, Maraviglia B, et al. Regional brain atrophy and functional disconnection across Alzheimer's disease evolution. J Neurol Neurosurg Psychiatry. 2011;82(1):58-66.
14. Gour N, Felician O, Didic M, Koric L, Gueriot C, Chanoine V, et al. Functional connectivity changes differ in early and late-onset Alzheimer's disease. Hum Brain Mapp. 2014;35(7):2978-94.
15. Dai Z, Yan C, Li K, Wang Z, Wang J, Cao M, et al. Identifying and Mapping Connectivity Patterns of Brain Network Hubs in Alzheimer's Disease. Cereb Cortex. 2015;25(10):3723-42.

16. Marchitelli R, Aiello M, Cachia A, Quarantelli M, Cavaliere C, Postiglione A, et al. Simultaneous resting-state FDG-PET/fMRI in Alzheimer Disease: Relationship between glucose metabolism and intrinsic activity. Neuroimage. 2018;176:246-58.
17. Tahmasian M, Pasquini L, Scherr M, Meng C, Forster S, Mulej Bratec S, et al. The lower hippocampus global connectivity, the higher its local metabolism in Alzheimer disease. Neurology. 2015;84(19):1956-63.
18. Teipel SJ, Metzger CD, Brosseron F, Buerger K, Brueggen K, Catak C, et al. Multicenter Resting State Functional Connectivity in Prodromal and Dementia Stages of Alzheimer's Disease. J Alzheimers Dis. 2018;64(3):801-13.
19. Wang J, Zuo X, Dai Z, Xia M, Zhao Z, Zhao X, et al. Disrupted functional brain connectome in individuals at risk for Alzheimer's disease. Biol Psychiatry. 2013;73(5):472-81.
20. Badhwar A, Tam A, Dansereau C, Orban P, Hoffstaedter F, Bellec P. Resting-state network dysfunction in Alzheimer's disease: A systematic review and meta-analysis. Alzheimers Dement (Amst). 2017;8:73-85.
21. Sheline YI, Raichle ME. Resting state functional connectivity in preclinical Alzheimer's disease. Biol Psychiatry. 2013;74(5):340-7.
22. Liu Y, Wang K, Yu C, He Y, Zhou Y, Liang M, et al. Regional homogeneity, functional connectivity and imaging markers of Alzheimer's disease: a review of resting-state fMRI studies. Neuropsychologia. 2008;46(6):1648-56.
23. Eyler LT, Elman JA, Hatton SN, Gough S, Mischel AK, Hagler DJ, et al. Resting State Abnormalities of the Default Mode Network in Mild Cognitive Impairment: A Systematic Review and Meta-Analysis. J Alzheimers Dis. 2019;70(1):107-20.
24. Joo SH, Lim HK, Lee CU. Three Large-Scale Functional Brain Networks from Resting-State Functional MRI in Subjects with Different Levels of Cognitive Impairment. Psychiatry Investig. 2016;13(1):1-7.
25. Koch K, Myers NE, Gottler J, Pasquini L, Grimmer T, Forster S, et al. Disrupted Intrinsic Networks Link Amyloid-beta Pathology and Impaired Cognition in Prodromal Alzheimer's Disease. Cereb Cortex. 2015;25(12):4678-88.
26. Zhou Y, Yu F, Duong TQ, Alzheimer's Disease Neuroimaging I. White matter lesion load is associated with resting state functional MRI activity and amyloid PET but not FDG in mild cognitive impairment and early Alzheimer's disease patients. J Magn Reson Imaging. 2015;41(1):102-9.
27. Mattsson N, Palmqvist S, Stomrud E, Vogel J, Hansson O. Staging β-Amyloid Pathology With Amyloid Positron Emission Tomography. JAMA Neurology. 2019;76(11):1319-29.
28. Elman JA, Madison CM, Baker SL, Vogel JW, Marks SM, Crowley S, et al. Effects of Beta-Amyloid on Resting State Functional Connectivity Within and Between Networks Reflect Known Patterns of Regional Vulnerability. Cereb Cortex. 2016;26(2):695-707.
29. Hedden T, Van Dijk KR, Becker JA, Mehta A, Sperling RA, Johnson KA, et al. Disruption of functional connectivity in clinically normal older adults harboring amyloid burden. J Neurosci. 2009;29(40):12686-94.

30. Sheline YI, Raichle ME, Snyder AZ, Morris JC, Head D, Wang S, et al. Amyloid plaques disrupt resting state default mode network connectivity in cognitively normal elderly. Biol Psychiatry. 2010;67(6):584-7.
31. Drzezga A, Becker JA, Van Dijk KR, Sreenivasan A, Talukdar T, Sullivan C, et al. Neuronal dysfunction and disconnection of cortical hubs in non-demented subjects with elevated amyloid burden. Brain. 2011;134(Pt 6):1635-46.
32. Lim HK, Nebes R, Snitz B, Cohen A, Mathis C, Price J, et al. Regional amyloid burden and intrinsic connectivity networks in cognitively normal elderly subjects. Brain. 2014;137(Pt 12):3327-38.
33. Mormino EC, Smiljic A, Hayenga AO, Onami SH, Greicius MD, Rabinovici GD, et al. Relationships between beta-amyloid and functional connectivity in different components of the default mode network in aging. Cereb Cortex. 2011;21(10):2399-407.
34. Jones DT, Knopman DS, Gunter JL, Graff-Radford J, Vemuri P, Boeve BF, et al. Cascading network failure across the Alzheimer's disease spectrum. Brain. 2016;139(2):547-62.
35. Wang Y, Risacher SL, West JD, McDonald BC, Magee TR, Farlow MR, et al. Altered default mode network connectivity in older adults with cognitive complaints and amnestic mild cognitive impairment. J Alzheimers Dis. 2013;35(4):751-60.
36. Sun Y, Dai Z, Li Y, Sheng C, Li H, Wang X, et al. Subjective Cognitive Decline: Mapping Functional and Structural Brain Changes-A Combined Resting-State Functional and Structural MR Imaging Study. Radiology. 2016;281(1):185-92.
37. Vega JN, Zurkovsky L, Albert K, Melo A, Boyd B, Dumas J, et al. Altered Brain Connectivity in Early Postmenopausal Women with Subjective Cognitive Impairment. Front Neurosci. 2016;10:433.
38. Dillen KNH, Jacobs HIL, Kukolja J, Richter N, von Reutern B, Onur OA, et al. Functional Disintegration of the Default Mode Network in Prodromal Alzheimer's Disease. J Alzheimers Dis. 2017;59(1):169-87.
39. Kawagoe T, Onoda K, Yamaguchi S. Subjective memory complaints are associated with altered resting-state functional connectivity but not structural atrophy. Neuroimage Clin. 2019;21:101675.
40. Hafkemeijer A, Altmann-Schneider I, Oleksik AM, van de Wiel L, Middelkoop HA, van Buchem MA, et al. Increased functional connectivity and brain atrophy in elderly with subjective memory complaints. Brain Connect. 2013;3(4):353-62.
41. Yasuno F, Kazui H, Yamamoto A, Morita N, Kajimoto K, Ihara M, et al. Resting-state synchrony between the retrosplenial cortex and anterior medial cortical structures relates to memory complaints in subjective cognitive impairment. Neurobiol Aging. 2015;36(6):2145-52.
42. Dong C, Liu T, Wen W, Kochan NA, Jiang J, Li Q, et al. Altered functional connectivity strength in informant-reported subjective cognitive decline: A resting-state functional magnetic resonance imaging study. Alzheimers Dement (Amst). 2018;10:688-97.
43. Verfaillie SCJ, Pichet Binette A, Vachon-Presseau E, Tabrizi S, Savard M, Bellec P, et al. Subjective Cognitive Decline Is Associated With Altered Default Mode Network Connectivity in Individuals With a Family History of Alzheimer's Disease. Biol Psychiatry Cogn Neurosci Neuroimaging. 2018;3(5):463-72.

44. Viviano RP, Hayes JM, Pruitt PJ, Fernandez ZJ, van Rooden S, van der Grond J, et al. Aberrant memory system connectivity and working memory performance in subjective cognitive decline. Neuroimage. 2019;185:556-64.
45. Chiesa PA, Cavedo E, Vergallo A, Lista S, Potier MC, Habert MO, et al. Differential default mode network trajectories in asymptomatic individuals at risk for Alzheimer's disease. Alzheimers Dement. 2019;15(7):940-50.
46. Li K, Luo X, Zeng Q, Jiaerken Y, Xu X, Huang P, et al. Aberrant functional connectivity network in subjective memory complaint individuals relates to pathological biomarkers. Transl Neurodegener. 2018;7:27.
47. Jessen F, Spottke A, Boecker H, Brosseron F, Buerger K, Catak C, et al. Design and first baseline data of the DZNE multicenter observational study on predementia Alzheimer's disease (DELCODE). Alzheimers Res Ther. 2018;10(1):15.
48. Palmqvist S, Scholl M, Strandberg O, Mattsson N, Stomrud E, Zetterberg H, et al. Earliest accumulation of beta-amyloid occurs within the default-mode network and concurrently affects brain connectivity. Nat Commun. 2017;8(1):1214.
49. Jack CR, Jr., Knopman DS, Jagust WJ, Shaw LM, Aisen PS, Weiner MW, et al. Hypothetical model of dynamic biomarkers of the Alzheimer's pathological cascade. Lancet Neurol. 2010;9(1):119-28.
50. Folstein MF, Folstein SE, Mchugh PR. “Mini-mental state”. a practical method for grading the cognitive state of patients for the clinician. J Psychiatr Res. 1975;12(3):189-98.
51. Mohs RC, Knopman D, Petersen RC, Ferris SH, Ernesto C, Grundman M, et al. Development of cognitive instruments for use in clinical trials of antidementia drugs: additions to the Alzheimer's Disease Assessment Scale that broaden its scope. The Alzheimer's Disease Cooperative Study. Alzheimer Dis Assoc Disord. 1997;11 Suppl 2:S13-21.
52. Seibyl J, Catafau AM, Barthel H, Ishii K, Rowe CC, Leverenz JB, et al. Impact of Training Method on the Robustness of the Visual Assessment of 18F-Florbetaben PET Scans: Results from a Phase-3 Study. J Nucl Med. 2016;57(6):900-6.
53. Ashburner J, Friston KJ. Unified segmentation. Neuroimage. 2005;26(3):839-51.
54. Tzourio-Mazoyer N, Landeau B, Papathanassiou D, Crivello F, Etard O, Delcroix N, et al. Automated anatomical labeling of activations in SPM using a macroscopic anatomical parcellation of the MNI MRI single-subject brain. Neuroimage. 2002;15(1):273-89.
55. Barthel H, Gertz HJ, Dresel S, Peters O, Bartenstein P, Buerger K, et al. Cerebral amyloid-beta PET with florbetaben (18F) in patients with Alzheimer's disease and healthy controls: a multicentre phase 2 diagnostic study. Lancet Neurol. 2011;10(5):424-35.
56. Yan CG, Wang XD, Zuo XN, Zang YF. DPABI: Data Processing & Analysis for (Resting-State) Brain Imaging. Neuroinformatics. 2016;14(3):339-51.
57. Friston KJ, Williams S, Howard R, Frackowiak RS, Turner R. Movement-related effects in fMRI time-series. Magn Reson Med. 1996;35(3):346-55.

58. Power JD, Barnes KA, Snyder AZ, Schlaggar BL, Petersen SE. Spurious but systematic correlations in functional connectivity MRI networks arise from subject motion. Neuroimage. 2012;59(3):2142-54.
59. Ashburner J. A fast diffeomorphic image registration algorithm. Neuroimage. 2007;38(1):95-113.
60. Zou QH, Zhu CZ, Yang Y, Zuo XN, Long XY, Cao QJ, et al. An improved approach to detection of amplitude of low-frequency fluctuation (ALFF) for resting-state fMRI: fractional ALFF. J Neurosci Methods. 2008;172(1):137-41.
61. Philip NS, Kuras YI, Valentine TR, Sweet LH, Tyrka AR, Price LH, et al. Regional homogeneity and resting state functional connectivity: associations with exposure to early life stress. Psychiatry Res. 2013;214(3):247-53.
62. Zang Y, Jiang T, Lu Y, He Y, Tian L. Regional homogeneity approach to fMRI data analysis. Neuroimage. 2004;22(1):394-400.
63. Zuo XN, Di Martino A, Kelly C, Shehzad ZE, Gee DG, Klein DF, et al. The oscillating brain: complex and reliable. Neuroimage. 2010;49(2):1432-45.
64. Zang YF, He Y, Zhu CZ, Cao QJ, Sui MQ, Liang M, et al. Altered baseline brain activity in children with ADHD revealed by resting-state functional MRI. Brain Dev. 2007;29(2):83-91.
65. Buckner RL, Sepulcre J, Talukdar T, Krienen FM, Liu H, Hedden T, et al. Cortical hubs revealed by intrinsic functional connectivity: mapping, assessment of stability, and relation to Alzheimer's disease. J Neurosci. 2009;29(6):1860-73.
66. Li S, Ma X, Huang R, Li M, Tian J, Wen H, et al. Abnormal degree centrality in neurologically asymptomatic patients with end-stage renal disease: A resting-state fMRI study. Clin Neurophysiol. 2016;127(1):602-9.
67. Mintun MA, Larossa GN, Sheline YI, Dence CS, Lee SY, Mach RH, et al. [11C]PIB in a nondemented population: potential antecedent marker of Alzheimer disease. Neurology. 2006;67(3):446-52.
68. Huijbers W, Mormino EC, Wigman SE, Ward AM, Vannini P, McLaren DG, et al. Amyloid deposition is linked to aberrant entorhinal activity among cognitively normal older adults. J Neurosci. 2014;34(15):5200-10.
69. Sheline YI, Morris JC, Snyder AZ, Price JL, Yan Z, D'Angelo G, et al. APOE4 allele disrupts resting state fMRI connectivity in the absence of amyloid plaques or decreased CSF Abeta42. J Neurosci. 2010;30(50):17035-40.
70. Filippini N, MacIntosh BJ, Hough MG, Goodwin GM, Frisoni GB, Smith SM, et al. Distinct patterns of brain activity in young carriers of the APOE-epsilon4 allele. Proc Natl Acad Sci U S A. 2009;106(17):7209-14.
71. Cohen AD, Price JC, Weissfeld LA, James J, Rosario BL, Bi W, et al. Basal cerebral metabolism may modulate the cognitive effects of Abeta in mild cognitive impairment: an example of brain reserve. J Neurosci. 2009;29(47):14770-8.
72. Schultz AP, Chhatwal JP, Hedden T, Mormino EC, Hanseeuw BJ, Sepulcre J, et al. Phases of Hyperconnectivity and Hypoconnectivity in the Default Mode and Salience Networks Track with Amyloid and Tau in Clinically Normal Individuals. J Neurosci. 2017;37(16):4323-31.

73. Hahn A, Strandberg TO, Stomrud E, Nilsson M, van Westen D, Palmqvist S, et al. Association Between Earliest Amyloid Uptake and Functional Connectivity in Cognitively Unimpaired Elderly. Cereb Cortex. 2019;29(5):2173-82.
74. Greicius MD, Srivastava G, Reiss AL, Menon V. Default-mode network activity distinguishes Alzheimer's disease from healthy aging: evidence from functional MRI. Proc Natl Acad Sci U S A. 2004;101(13):4637-42.
75. Bero AW, Yan P, Roh JH, Cirrito JR, Stewart FR, Raichle ME, et al. Neuronal activity regulates the regional vulnerability to amyloid-beta deposition. Nat Neurosci. 2011;14(6):750-6.
76. Cirrito JR, Yamada KA, Finn MB, Sloviter RS, Bales KR, May PC, et al. Synaptic activity regulates interstitial fluid amyloid-beta levels in vivo. Neuron. 2005;48(6):913-22.
77. Leech R, Sharp DJ. The role of the posterior cingulate cortex in cognition and disease. Brain. 2014;137(Pt 1):12-32.
78. Morris JC, Roe CM, Xiong C, Fagan AM, Goate AM, Holtzman DM, et al. APOE predicts amyloid-beta but not tau Alzheimer pathology in cognitively normal aging. Annals of Neurology. 2010;67(1):122-31.
79. Hafkemeijer A, van der Grond J, Rombouts SA. Imaging the default mode network in aging and dementia. Biochim Biophys Acta. 2012;1822(3):431-41.
80. Buckley RF, Schultz AP, Hedden T, Papp KV, Hanseeuw BJ, Marshall G, et al. Functional network integrity presages cognitive decline in preclinical Alzheimer disease. Neurology. 2017;89(1):29-37.
81. Cavedo E, Chiesa PA, Houot M, Ferretti MT, Grothe MJ, Teipel SJ, et al. Sex differences in functional and molecular neuroimaging biomarkers of Alzheimer's disease in cognitively normal older adults with subjective memory complaints. Alzheimers Dement. 2018;14(9):1204-15.
82. Bullich S, Seibyl J, Catafau AM, Jovalekic A, Koglin N, Barthel H, et al. Optimized classification of 18F-Florbetaben PET scans as positive and negative using an SUVR quantitative approach and comparison to visual assessment. NeuroImage: Clinical. 2017;15:325-32.

Tables

Table 1: Sample characteristics and regional amyloid tracer uptake for the amyloid-positive and -negative subgroups

	$SCD_{A\beta+}$	$SCD_{A\beta-}$	Test Statistics	P value
Age (yrs)	74.54 ± 4.40	74.04 ± 4.13	t(46) = 0.41	0.69
Gender (F/M)	9/15	9/15	χ^2 (1) = 0.00	1
Education (yrs)	14.42 ± 2.78	14.96 ± 3.36	t(46) = 0.61	0.55
MMSE	29.13 ± 0.90*	29.00 ± 1.44*	U(46) = 247.50	0.69
ADAS-cog13	8.38 ± 3.68	7.25 ± 3.27	t(46) = 1.12	0.27
APOE(*ε4/non-4*)	17/6*	6/17*	χ^2 (1) = 10.52	0.001
Global $SUVR_{FBB}$	1.79 ± 0.25	1.32 ± 0.10	t(46) = 8.38	<0.001
Precuneus $SUVR_{FBB}$	1.92 ± 0.31	1.29 ± 0.07	t(46) = 9.74	<0.001

*: Denotes 1 missing value.

Abbreviations: $SCD_{Aß+}$ = Amyloid-positive subjective cognitive decline group, $SCD_{Aß-}$ = amyloid-negative subjective cognitive decline group; U= Whitney U value; MMSE Mini-Mental -State Examination; ADAS-cog13 Alzheimer's Disease Assessment Scale—cognitive part; APOE: Apolipoprotein; SUVR=Standard Uptake Value Ratio with cerebellar cortex as reference region; FBB= [18F]-Florbetaben. Continuous data are presented as means ± standard deviations.

Table 2: Brain regions showing increased regional homogeneity in amyloid-positive compared to amyloid-negative SCD participants

Cluster Size	P value (FWE)	Brain Regions	Peak MNI Coordinate			Peak T Value
			x	y	z	
270	0.034	Right precuneus	6	-54	69	4.34
		Left superior parietal lobule	-18	-54	72	3.75
		Right superior parietal lobule	15	-63	66	3.63

Abbreviations: FWE – Family-wise error. MNI – Montreal Neurological Institute.

Table 3: Brain regions showing increased precuneus-based functional connectivity in amyloid-positive compared to amyloid-negative SCD participants

Cluster Size	P value (FWE)	Brain Regions	Peak MNI Coordinate			Peak T Value
			x	y	z	
296	< 0.001	Right middle occipital gyrus	27	-75	30	3.95
		Right cuneus	12	-87	42	3.62
		Right superior occipital_gyrus	27	-84	21	3.17

Abbreviations: FWE – Family-wise error. MNI – Montreal Neurological Institute.

Figures

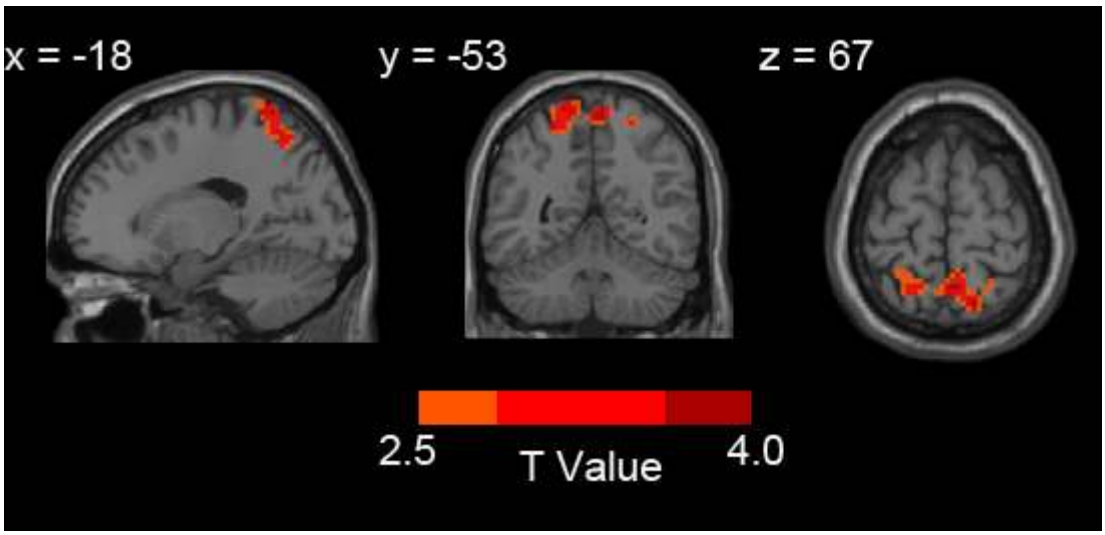

Figure 1

Brain regions showing increased ReHo in SCDAß+ compared to SCDAß- The figure shows the regions with significant increased ReHo value in SCDAβ+ compared to SCDAβ- (p < 0.05, FWE cluster-level). The color bar represents the heights of suprathreshold t-values.

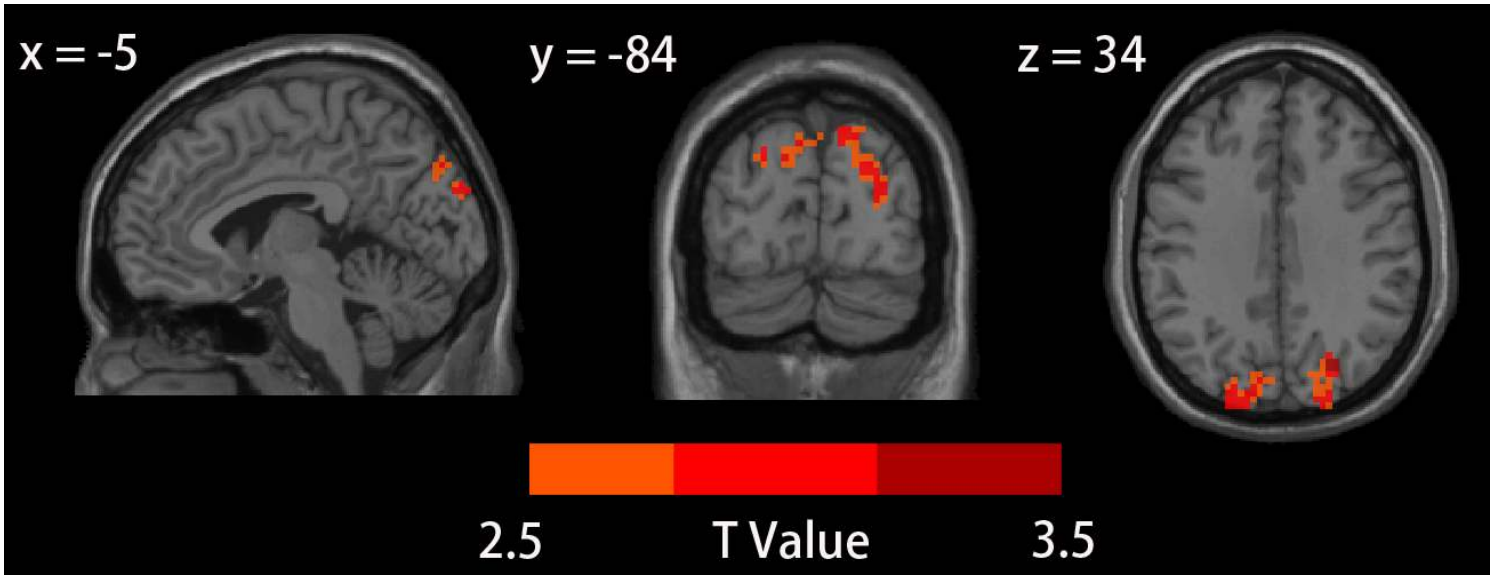

Figure 2

Brain regions showing increased precuneus-based FC in SCDAβ+ compared to SCD Aβ- The figure represents increased voxel-wise FC of the precuneus seed region with the cuneus and superior/middle occipital regions in the SCDAß+ group ($p < 0.05$, FWE cluster-level). The color bar represents the height of suprathreshold t-values.

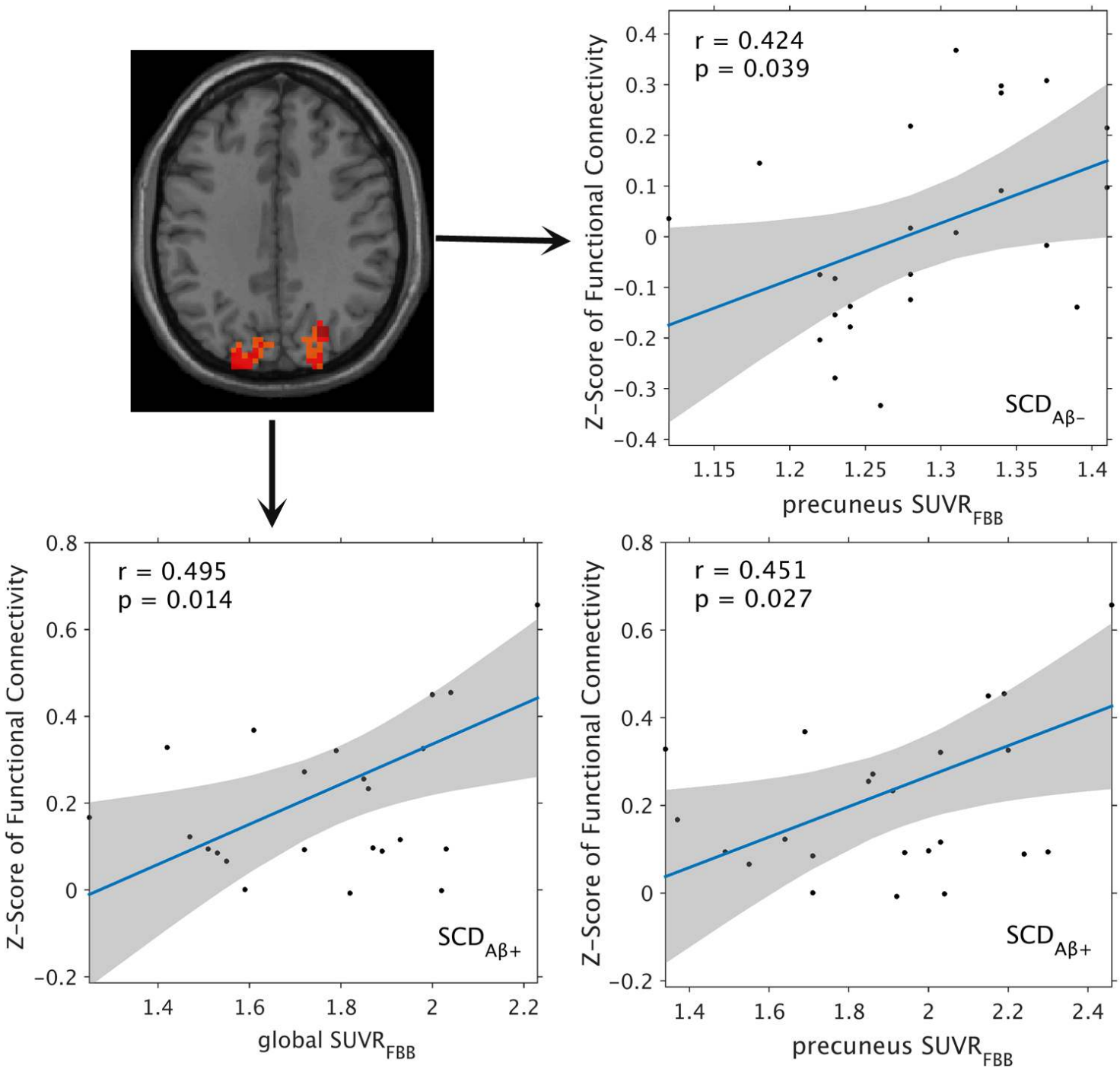

Figure 3

Positive correlations between increased precuneus FC with occipital regions and global SUVRFBB and precuneus SUVRFBB The grey regions are 95% confidential intervals. The mean Z-Score of the FC was extracted from significant cluster within the red circle. Abbreviations: SCDAβ+ - amyloid-positive SCD; SCDAβ- - amyloid-negative SCD; SUVR=Standard Uptake Value Ratio (with cerebellar cortex as reference region).

Supplementary Files

This is a list of supplementary files associated with this preprint. Click to download.

- AdditionalFile1.docx